Analysis of an Unusually Strong Supercell That Impacted the Mission Valley of Western Montana on July 18, 2007

Bridget M. De Rosa
National Weather Service
WFO Missoula, MT

1. Introduction

Severe thunderstorms developed in north central Idaho during the late afternoon of July 18, 2007 and tracked across western Montana during the evening hours. Despite the dry conditions and record-breaking heat observed across the region during July 2007, several atmospheric elements and conditions came together to provide a focus for splitting supercells and enhanced storm rotation. A strong and long-lived supercell formed east of Superior, MT after the leading thunderstorm of the day split, and the right-moving cell merged with the storm behind it. The supercell and associated mesocyclone (Figure 1) gained strength upon entering the Mission Valley (Figure 2) and tracked northeast toward Polson, MT and over Flathead Lake before weakening. Although tornado damage was inconclusive during the National Weather Service (NWS) storm survey, funnel clouds and a waterspout were reported over Flathead Lake near Polson with this particular supercell. This case study will evaluate the sequence of events that led to this unusually strong supercell and mesocyclone.

2. Pre-Storm Environment

Because of the hot and dry conditions experienced throughout the summer of 2007, the Global Forecast System (GFS) model was the preferred guidance data due to its dry bias during the summer months. On July 18, 2007, the GFS model retained its dry bias despite abundant low-level atmospheric moisture across the region that day. This may have skewed the forecast on July 18th, since (per the GFS) the influx of subtropical moisture was not expected to occur until the overnight hours; enhancing the potential for nocturnal thunderstorm development instead. Exploring model performance is not the intention of this case study, and no further mention will be made.

The focus of model interrogation turns to the North American Mesoscale (NAM12) model data. NAM12 data represented low-level atmospheric moisture and the generation of late day convective precipitation much better than the GFS on this particular day. The 1200 UTC NAM12 model run presented an ideal set-up for convection in western Montana based on plan view data and model soundings and will be reviewed respectively.

Model Data

A strong upper-level ridge of high pressure over the Northern Rockies of Montana was breaking down, as a trough along the northern California/Oregon coast pushed inland. This scenario allowed for increased moisture and increasing south-southwest flow above 700 mb over the Missoula County Warning Area (CWA) (Figure 3). With a thermal surface trough progged directly over western Montana during peak heating, this was a favorable synoptic weather pattern for low-level convergence and increased thunderstorm development. Also of note are the southeast 850 mb winds seen in Figure 4 at 18/2100 UTC. Surface METAR/LDAD observations at 19/0000 UTC showed strong southeast winds along the Interstate 90 (I-90) corridor through Missoula and light northwest winds in northwest Montana and the Mission Valley (Figure 5). The predicted 850 mb winds and surface observations imply that a pseudo-warm frontal feature was present with a potential convergence zone in the southern Mission Valley, which could provide a focusing mechanism for storm initiation. This would not be the case on this particular day, and will be explained further in Section 3 entitled *Supercell Evolution*. Overall, the southeast surface wind orientation combined with the strong south-southwest winds aloft indicated that winds were veering with height and that conditions were ideal for rotating thunderstorms.

Sounding Data and Additional Convective Parameters

In evaluating available low-level moisture, the morning of July 18, 2007 began with fog in most valleys of north central Idaho and western Montana as a result of convective rainfall the previous evening. This helped to prime the lower levels of the atmosphere with moisture as indicated by morning surface dewpoints in the low to mid 50s, which is high for western Montana. Upper air observations taken at 18/1200 UTC from Spokane, WA and Boise, ID both indicated that strong surface inversions were in place with a weaker cap aloft at roughly 750 mb (Figure 6a and 6b respectively). The presence of surface inversions and the weaker cap aloft would prevent the low-level moisture from evaporating too quickly as temperatures soared into the upper 90s and low 100s that afternoon. Hodographs for Kalispell, MT (KGPI – not shown) and Missoula, MT (KMSO) (Figure 7) indicated a clockwise curvature from the surface to roughly 4 km above ground level (AGL). Per Klemp and Wilhelmson (1978), the hodograph curvatures implied that right-moving storms would be predominant once thunderstorms initiated.

Using 18/1200 UTC model data, NAM12 soundings for KMSO, KGPI and near Thompson Falls, MT (S06) indicated favorable instability parameters for convective potential and type of convection anticipated during the late afternoon and evening hours of July 18th. A veering shear profile with height and vertical wind shear values of 25-40 kt over the lowest 0-6 km above ground level (AGL) implied that the environment was conducive to supercell development (WDTB, 2010a). These parameter values were also more than sufficient to support a strong, tilted updraft as well as mid-level rotation of the updraft once thunderstorms initiated. An unmodified NAM12 1800 UTC sounding for KMSO at 19/0000 UTC indicated a Bulk Richardson Number of approximately 62, whereas values in the 10-40 range support an environment suitable for supercell development (COMET, 1997). Inverted-V profiles progged at 19/0000 UTC indicated the potential for microbursts with surface $T\text{-}T_d$ spreads of 40-55 ^{o}F, where local minimum criterion for microbursts is 45 ^{o}F. NAM12 soundings also showed a relatively high lifted condensation level (LCL) located at approximately 10-14.5 kft mean sea level (MSL) and "a deep dry adiabatic layer [from the LCL] down to the surface in order for the downdraft to reach the ground (WDTB, 2010b, pp. 7-51 – 7-52). Actual $T\text{-}T_d$

spreads were observed to be 40-50 ^{o}F on average across the Missoula CWA. Precipitable water values were in excess of 1.00 inch (150% of normal for the Missoula CWA at 18/1200 UTC), thus wet microbursts could be favored over dry microbursts on this day. In addition, convective available potential energy (CAPE) above 3000 J/kg (above 2200 J/kg on modified soundings), convective inhibition (CIN) near 0 J/kg, lifted index values of -3 to -6 ^{o}C, and steepening lapse rates approaching 8.5 ^{o}C/km in the 850-500 mb layer were all favorable instability parameters for convection that could be realized if the mid-level cap were to break (particularly during peak heating).

NAM12 soundings progged at 18/2100 UTC for the same locations suggested that the mid-level capping inversion would erode between 18/2100 and 19/0000 UTC (Figure 8). With upper air observations and model soundings indicating the presence of a mid-level cap, and with surface temperatures warming sufficiently through the day, this situation was not a matter of, "Will the cap break?" but a matter of, "When will the cap break?" in order to realize the potential instability present.

3. Supercell Evolution

Valley fog had dissipated in area valleys between 18/1500 and 18/1600 UTC, giving way to mostly clear skies for the rest of the day. Despite numerous wildfires burning in central Idaho, smoke plumes had a negligible shadowing effect on July 18th. As a result, this would allow surface heating to be fully realized on this day. Rapid surface temperature rises of 4+ ^{o}F observed every hour after the fog dissipated at KMSO and KGPI indicated that the mid-level cap was firmly in place over western Montana (McGinley, 1986). By the mid-afternoon hours, slower surface temperature rises of 2-3 ^{o}F were observed at KMSO and KGPI (18/2000-18/2100 UTC and 18/2100-18/2200 UTC respectively), thus indicating that the mid-level capping inversion had broken at the aforementioned locations. Once this happened, cumulus clouds developed quickly over the Clearwater Mountains in Idaho (Figure 9).

A subtle shortwave feature was also moving northward; helping to trigger the thunderstorms that would impact western Montana during the evening hours of July 18th. The shortwave was difficult to discern on water vapor imagery, therefore NAM12 vertical wind shear values in the 700-400 mb layer were examined (particularly during peak heating). Using this procedure, 700 mb was the lowest layer chosen in order to alleviate terrain influences during model analysis. Weisman and Klemp (1986) stated that supercell thunderstorms owe their existence to dynamically induced pressure forces, which result when vertical wind shear extends through the mid-levels of a storm (approximately 4-6 km AGL). As such, evaluation of the layer data in this procedure shows that shortwaves are located where the vertical wind shear values are at a maximum. As seen in Figure 10, maximum values of 40-42 kt at 19/0000 UTC were indicating the presence of a shortwave feature over western Montana, which would ultimately trigger thunderstorms during the late afternoon on July 18th.

The first convective radar returns were detected by WSR-88D KMSX at 18/2156 UTC east of Elk City, ID. A line of convection quickly developed in a north-south orientation, and by 18/2322 UTC, a separate storm was forming north of Powell, ID in the northern Bitterroot

Mountains (Figure 11). This particular storm cell (J0) would intensify quickly and move northward as well.

Before proceeding further into radar interrogation, it is important to note the volume coverage pattern (VCP) applied to WSR-88D KMSX throughout this event. VCP 21 was used as the coverage choice. VCP 21 is best used during non-severe convective precipitation and completes a full volume scan in six minutes. VCP 12 would have been preferred in this case, as it is well-suited for severe convective events, samples more low-level elevation angles, and completes a full volume scan in four and a half minutes as compared to VCP 21. With convection spinning up quickly the afternoon of July 18, 2007 and with limited staff coverage during an evening shift, the use of VCP 21 was an oversight. However, this was not a detriment to the evaluation of this particular supercell, since it was close enough to the radar to allow for ample data sampling. Regardless of the VCP used during this event, the lowest level of radar data could only be sampled as low as 4000-7000 ft AGL throughout the storm's lifecycle. This is due to the location of WSR-88D KMSX on Point 6 Mountain at an elevation of 7929 ft MSL. For the purpose of this case study, storm motion was customized to 210^{o} at 37 kt for this specific supercell.

At 19/0021 UTC, the J0 cell showed signs of splitting into a right- and left-moving storm. Meanwhile, another storm cell (H0) was moving northward behind J0, gaining strength, and veering toward the right on its northward track. The H0 storm produced 1.75 inch diameter hail near Tarkio, MT at 19/0044 UTC. The right-moving cell from J0 would merge with the H0 storm and form a new supercell (H0 – known as the Polson supercell hereafter) near Perma, MT by 19/0056 UTC per the SCAN Storm Cells graphic in AWIPS (Figure 12).

4. Supercell Lifecycle

The Polson supercell would quickly intensify upon entering the Mission Valley. Dewpoint values in the mid 50s to low 60s across the Mission Valley during the late afternoon hours suggested that enhanced low-level moisture was present, which would support updraft growth (Weisman & Klemp, 1986) and aid in the supercell's longevity as it tracked across this area. Low-level base reflectivity cores (0.5^{o} and 1.5^{o}) at 19/0033 UTC were showing the first signs of a strengthening updraft with values of 66.5 dBZ at 5769 and 9465 feet AGL respectively. The updraft would remain strong during the storm's lifecycle with values of 65-72 dBZ throughout the low and mid-levels of the storm until roughly 19/0231 UTC.

Cyclonic rotation quickly became evident on Storm Relative Motion (SRM) data in the mid-levels of the supercell by 19/0108 UTC. Cyclonic rotation would intensify down to the lowest levels of the storm by 19/0119 UTC just east of Perma, at which time the first of three WSR-88D algorithm Tornadic Vortex Signature (TVS) alarms would be triggered. Horizontal gate-to-gate shear values were increasing with height: 48 kt at 0.5^{o}, 71 kt at 1.5^{o} and an impressive 98 kt at 2.4^{o} (Figure 13). The base velocity 4-panel image during the same time (not shown) displays an identical cyclonic rotation image as compared to the SRM 4-panel data with the following inbound (-) and outbound values (+): -31/20 kt at 0.5^{o}, -37/39 kt at 1.5^{o}, -33/62 kt at 2.4^{o} and -35/32 at 3.4^{o}. A well-defined and deep mesocyclone was also unmistakable at the middle and upper levels of the supercell's storm structure at 19/0119 UTC. Figure 14 best represents the mesocyclone and strong storm top divergence seen in this particular 4-panel base velocity image. Strong mid-level SRM cyclonic rotation at 6.0^{o} with 68 kt of horizontal gate-to-gate shear was also observed at this time.

Moving forward in time to 19/0132 UTC, cyclonic rotation of the mesocyclone remained strong, and storm top divergence at 10.0^{o} was exceptionally robust with 141 kt of total shear velocity (not shown). Inflow notches were seen through the height of the storm at this time (0.5^{o}-6.0^{o}), as indicated by sharp reflectivity gradients on the southeast side of the supercell. Per Moller et al. (1990), this is a classic high precipitation (HP) supercell feature and further supports the presence of a strong updraft. The presence of inflow notches also reinforced that the microburst potential on this day was toward the wet end of the threat spectrum. Although there was no TVS alarm generated by the WSR-88D algorithm at this point, the cyclonic rotation signatures and associated shear values supported the issuance of a tornado warning at 19/0134 UTC. A tornado warning would be in effect for the remainder of the Polson supercell's lifecycle.

Some of the most impressive data seen during this case study occurs in the 19/0144 to 19/0156 UTC timeframe. Reflectivity cross sections show strong evidence of a microburst occurring in the Figure 15a-c sequence. At 19/0144 UTC, Figure 15a shows a classic image of a Bounded Weak Echo Region (BWER), which "indicates the presence of both strong updraft and strong rotation about a vertical axis in its vicinity (Weisman & Klemp, 1986, p. 336). The maximum height of the BWER was located just above 400 mb. Also of importance was the presence of an elevated reflectivity storm core just above 500 mb at this time. A second WSR-88D algorithm TVS alarm was triggered during this volume scan and continued during the next scan (19/0150 UTC) as well. At 19/0150 UTC, the BWER was collapsing as the elevated reflectivity core was intensifying (Figure 15b). By 19/0156 UTC (Figure 15c), the elevated reflectivity storm core was descending toward the surface and continued to intensify, which is a classic precursor signature of a microburst (WDTB, 2010b). The BWER had almost completely collapsed at this point as well. The combination of the collapsing BWER and the descending reflectivity core was potentially enhancing the strength of the microburst and the subsequent wind damage at the ground surface. It is important to note that collapsing BWERs have been known to correspond with tornado touchdowns (McGinley, 1986). As a result, the NWS storm survey team needed to determine whether wind damage that occurred a few miles west of Pablo during this time sequence was due to straight-line winds from a microburst or cyclonic winds from a tornado.

One hour after storm cells J0 and H0 merged to form the Polson supercell (19/0219 UTC), the storm structure was still exhibiting a strong updraft and tracking north-northeast in the vicinity of Polson and over Flathead Lake (Figure 16). Cyclonic rotation was still evident on base velocity 4-panel data and SRM 4-panel data as the supercell passed over the southwestern shores of Flathead Lake. Low-level SRM data at 0.5^{o} and 1.5^{o} had horizontal gate-to-gate shear values of 47 kt and 63 kt respectively. Meanwhile, inbound velocity values were increasing with height as the mesocyclone continued to extend through at least 2/3 of the storm height. A third WSR-88D algorithm TVS alarm was triggered at 19/0213 UTC and persisted for three volume scans (19/0213 to 19/0225 UTC), even though cyclonic rotation remained visible through the 19/0231 UTC radar volume scan.

The Polson supercell gave one last hurrah in the form of straight-line wind damage on the northern end of Flathead Lake. It is speculated that the wind damage experienced near Somers, MT between 19/0236 and 19/0300 UTC was a result of the supercell's collapsing downdraft and essentially resulted in a microburst occurring at the surface (Figure 17). By 19/0300 UTC, the Polson supercell and mesocyclone had weakened significantly as observed in decreased base velocity values and base reflectivities, and it was no longer severe.

5. Polson Supercell Storm Reports and Damage

The first storm report from the Polson supercell (i.e. after storm cells J0 and H0 merged and entered the Mission Valley) came from Perma at 19/0130 UTC in the form of 0.88 inch diameter hail and is noted in Figure 18, which shows a map of local storm reports for July 18, 2007. Fifteen to twenty minutes later, the Polson supercell would impact an area four miles west of Pablo (located southwest of Polson). Numerous reports of structural damage to metal barn structures (Figure 19), felled trees and limbs, 2 x 4 foot pieces of wood stuck several inches into the ground, and tipped over irrigation equipment were the main highlights of storm damage in this area.

As the supercell approached Polson and the western shores of Flathead Lake, storm reports of damage increased. This is probably due to the area around Flathead Lake having a larger population as compared to the southern portions of the Mission Valley near Perma or west of Pablo, which are more rural. At 19/0150 UTC, severe hail of 1.50 inches in diameter was reported ten miles west-northwest of Pablo. Ten to fifteen minutes after this hail report, the shoreline between Elmo, MT and Rollins, MT would incur wind damage as the supercell tracked along the western shores of Flathead Lake. In this area, docked boats were pushed up onto the shore (Figure 20), and numerous trees were completely uprooted and strewn in a unidirectional orientation (as photographed by the Lake County Department of Emergency Services and viewed during the NWS storm survey). Based on mainly tree damage observed across the Mission Valley region and utilizing the Enhanced Fujita Scale (Texas Tech University, 2004), winds were estimated to be in excess of 80 mph.

Several reports of funnel clouds over Flathead Lake were also received from 19/0158 to 19/0240 UTC. In addition, a waterspout was reported over Flathead Lake near Rollins during this time. A sailor encountered during the storm survey gave his account of being caught on a twenty-six foot sailboat as he and another gentleman tried to get the boat to safe harbor during the storm. The boat spun counterclockwise 360^{o} while the sailors were pelted with hail (large enough to leave bruises on the backs of their heads, necks and backs) and strong winds. Eventually they abandoned ship, the boat sank and the sailors were rescued from the water a few hours later by the Lake County Search and Rescue Organization.

Wind damage experienced near Somers (19/0231 to 19/0300 UTC) resulted from the supercell's collapsing downdraft and subsequent microburst (see Figure 17). In this area, a metal silo was knocked over and several metal barn structures were damaged (Figure 21 and

22 respectively). At one residence, a four to five foot diameter cottonwood tree was completely uprooted (Figure 23). Luckily, there was no damage to the residence.

6. Conclusion

Several factors led to the long-lived nature of the Polson supercell and mesocyclone. A favorable pre-storm environment with sufficient moisture, synoptic-scale instability, atmospheric lift and vertical wind shear helped to trigger rapidly developing thunderstorms during peak heating on July 18, 2007. In addition, the orientation of southeast surface winds and strong south-southwest winds aloft allowed for rotating storms to develop on this day. A very strong updraft aided in the longevity of the Polson supercell as evidenced by high reflectivity storm cores, inflow notches at multiple levels, and strong storm top divergence throughout the supercell's lifecycle. Also, cyclonic rotation of the deep and well-defined mesocyclone further enhanced the updraft and strength of the supercell as it tracked across the Mission Valley.

Evaluation of the radar data suggests that the combination of a mesocyclone, BWER and WSR-88D algorithm TVS alarms (WDTB, 2010c) supported the existence of isolated tornadoes with this supercell. Radar data also revealed the presence of descending reflectivity cores and collapsing BWERs, which strongly suggests that enhanced microbursts occurred; causing structural damage and downed trees at the ground surface. NWS storm survey evidence determined that straight-line winds from microbursts were the primary cause of storm damage at the surface and not from cyclonic winds associated with tornadoes. A few twisted branches were observed west of Pablo, where farmland and sparse population is commonplace. As a result, tornado confirmation was difficult to obtain.

7. Acknowledgements

The author would like to thank Chris Gibson for his guidance, wisdom and constructive comments throughout this process. The author would also like to thank Mark Mollner for his input regarding the final draft of this paper.

8. References

Burgess, D. & Lemon, L. (1990). Severe Thunderstorm Detection by Radar. In D. Atlas (Ed.), Radar in Meteorology (pp. 619-647). Boston: American Meteorological Society.

COMET Computer-based Module. (1997). Anticipating Convective Storm Structure and Evolution: Summary Page – Key Points to Remember. Retrieved from http://www.meted.ucar.edu/convectn/mod8sumpag.pdf.

Klemp, J., & Wilhelmson, R. (1978b). Simulations of right- and left-moving storms produced through storm splitting. Journal of Atmospheric Sciences, 35(6), 1097-1110.

Moller, A., C. A. Doswell, & R. Przybylinski. (1990). High-precipitation supercells: A conceptual model and documentation. Preprints, 16th Conf. Severe Local Storms, American Meteorological Society, Boston, 52-57.

McGinley, J. (1986). Nowcasting Mesoscale Phenomena. In P. Ray (Ed.), Mesoscale

Meteorology and Forecasting (pp. 657-688). Boston: American Meteorological Society.
Rotunno, R. (1986). Tornadoes and Tornadogenesis. In P. Ray (Ed.), Mesoscale Meteorology and Forecasting (pp. 414-436). Boston: American Meteorological Society.
Texas Tech University – Wind Science and Engineering Center. (2004). A Recommendation for an Enhanced Fujita Scale (EF-Scale). 2004. Retrieved from http://www.spc.noaa.gov/ faq/tornado/ef-ttu.pdf.
University of Wyoming. Upper Air Observations. Retrieved from http://weather.uwyo.edu/ upperair/sounding.html.
Warning Decision Training Branch (WDTB) – Distance Learning Operations Course (DLOC). (2010a). Supercell Dynamics. Retrieved from http://www.wdtb.noaa.gov/ courses/dloc/documentation/DLOC10-Topic7.pdf.
Warning Decision Training Branch (WDTB) – Distance Learning Operations Course (DLOC). (2010b). Single Cell Downbursts. Retrieved from http://www.wdtb.noaa.gov/courses/dloc/documentation/DLOC10-Topic7.pdf.
Warning Decision Training Branch (WDTB) – Distance Learning Operations Course (DLOC). (2010c). Tornado Hazards. Retrieved from http://www.wdtb.noaa.gov/ courses/dloc/documentation/DLOC10-Topic7.pdf.
Weisman, M., & Klemp, J. (1986). Characteristics of Isolated Convective Storms. In P. Ray (Ed.), Mesoscale Meteorology and Forecasting (pp. 331-358). Boston: American Meteorological Society.

9. Figures

Figure 1 – High precipitation (HP) supercell and mesocyclone as viewed in the Mission Valley of western Montana on July 18, 2007 (photo courtesy of the Lake County Sheriff). Notice the strong surface winds in the vicinity of the supercell; as indicated by the bending tree in the foreground of this image.

Figure 2 – Map of the Mission Valley in western Montana.

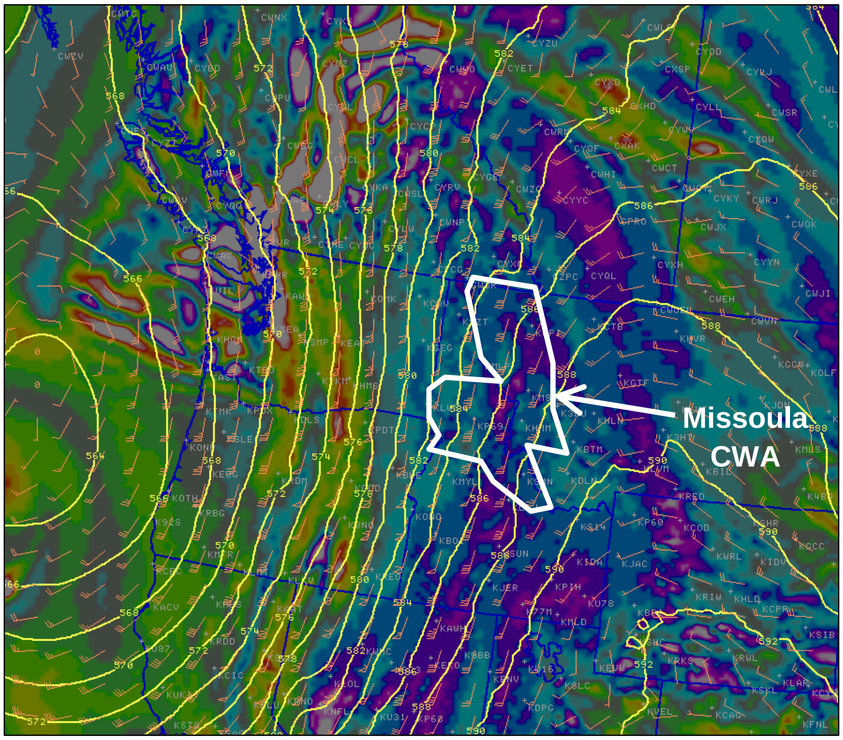

Figure 3 – NAM12 data progged at 19/0000 UTC and showing the upper ridge breaking down as the upper level trough moves onto the western coast of the United States. Seen here are 500 mb heights (yellow lines), 500 mb winds (orange wind barbs), a vorticity image, and a white outline of the Missoula County Warning Area (CWA).

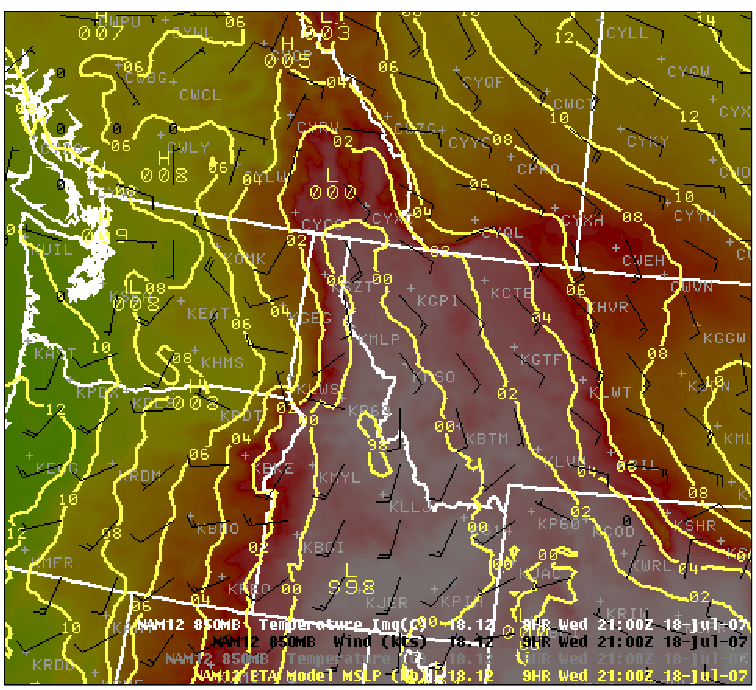

Figure 4 – NAM12 data progged at 18/2100 UTC and showing a thermal surface trough. Seen here are MSLP (yellow lines), 850 mb winds (black wind barbs) and an 850 mb temperature image.

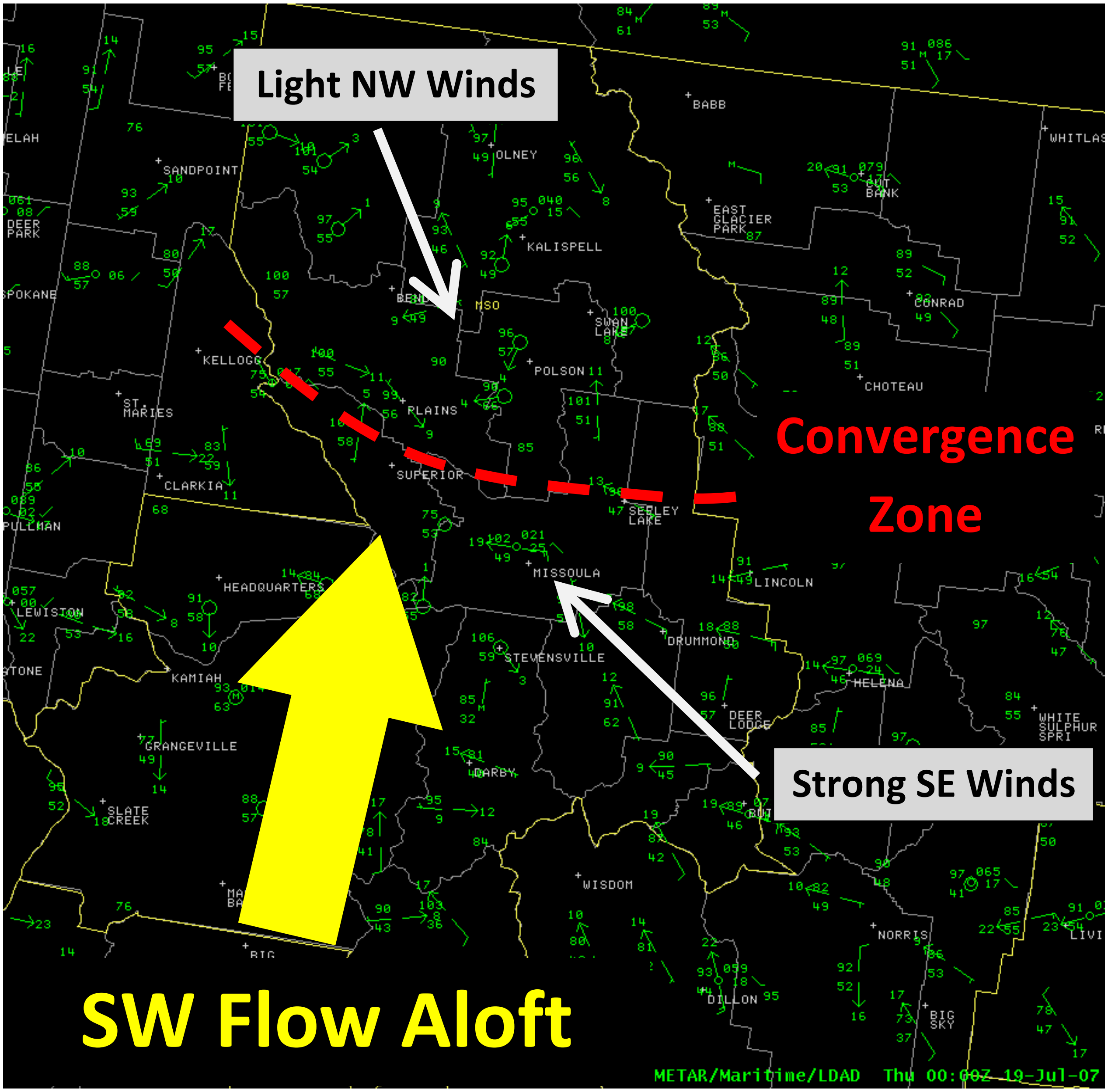

Figure 5 – Surface METAR/LDAD observations (green) at 19/0000 UTC. The presence of a pseudo-warm frontal boundary (and associated convergence zone) is inferred based on surface wind directions. Strong south-southwest winds aloft indicated that winds were veering with height, and that conditions were ideal for rotating thunderstorms.

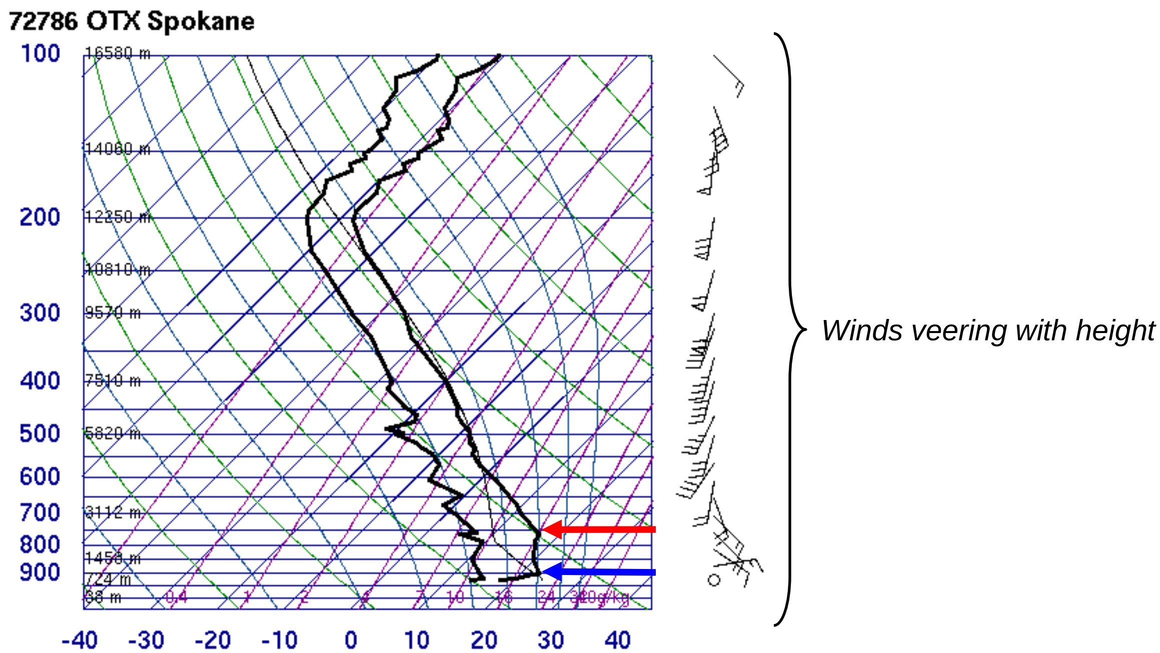

Figure 6a – 18/1200 UTC upper air observations for Spokane, WA (courtesy of the University of Wyoming). Conditions on the morning of July 18th show a surface inversion (blue arrow), and a weaker inversion at approximately 750 mb (red arrow), which would "cap" the atmosphere until late afternoon.

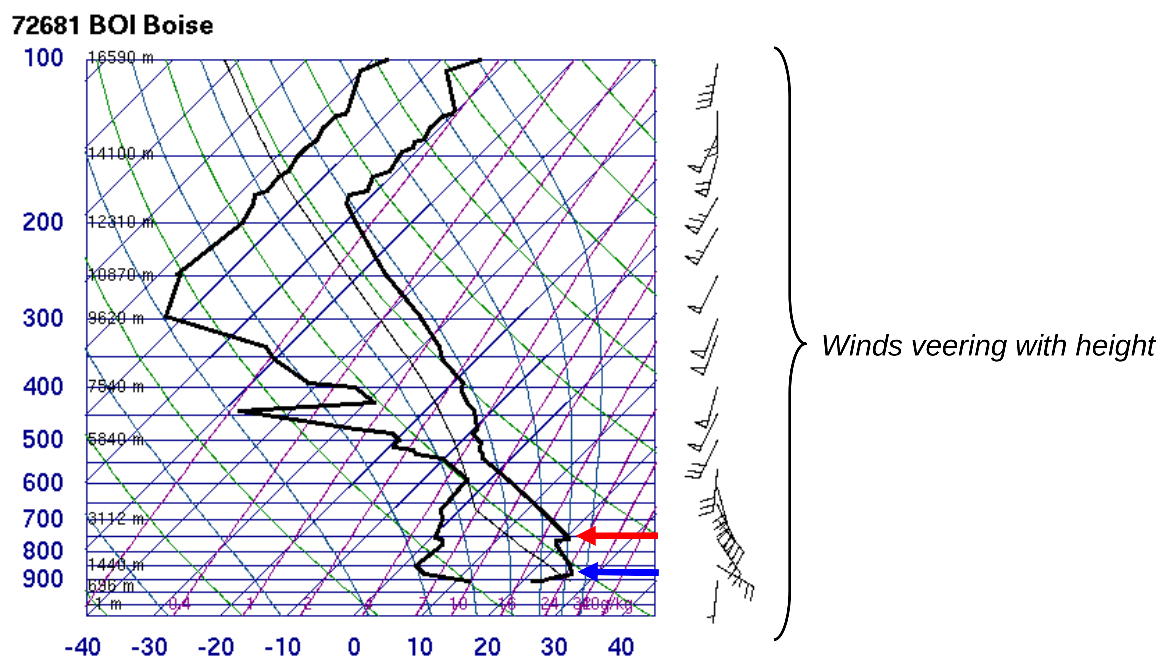

Figure 6b – 18/1200 UTC upper air observations for Boise, ID (courtesy of the University of Wyoming). Conditions on the morning of July 18th show a surface inversion (blue arrow), and a weaker inversion at approximately 750 mb (red arrow), which would "cap" the atmosphere until late afternoon.

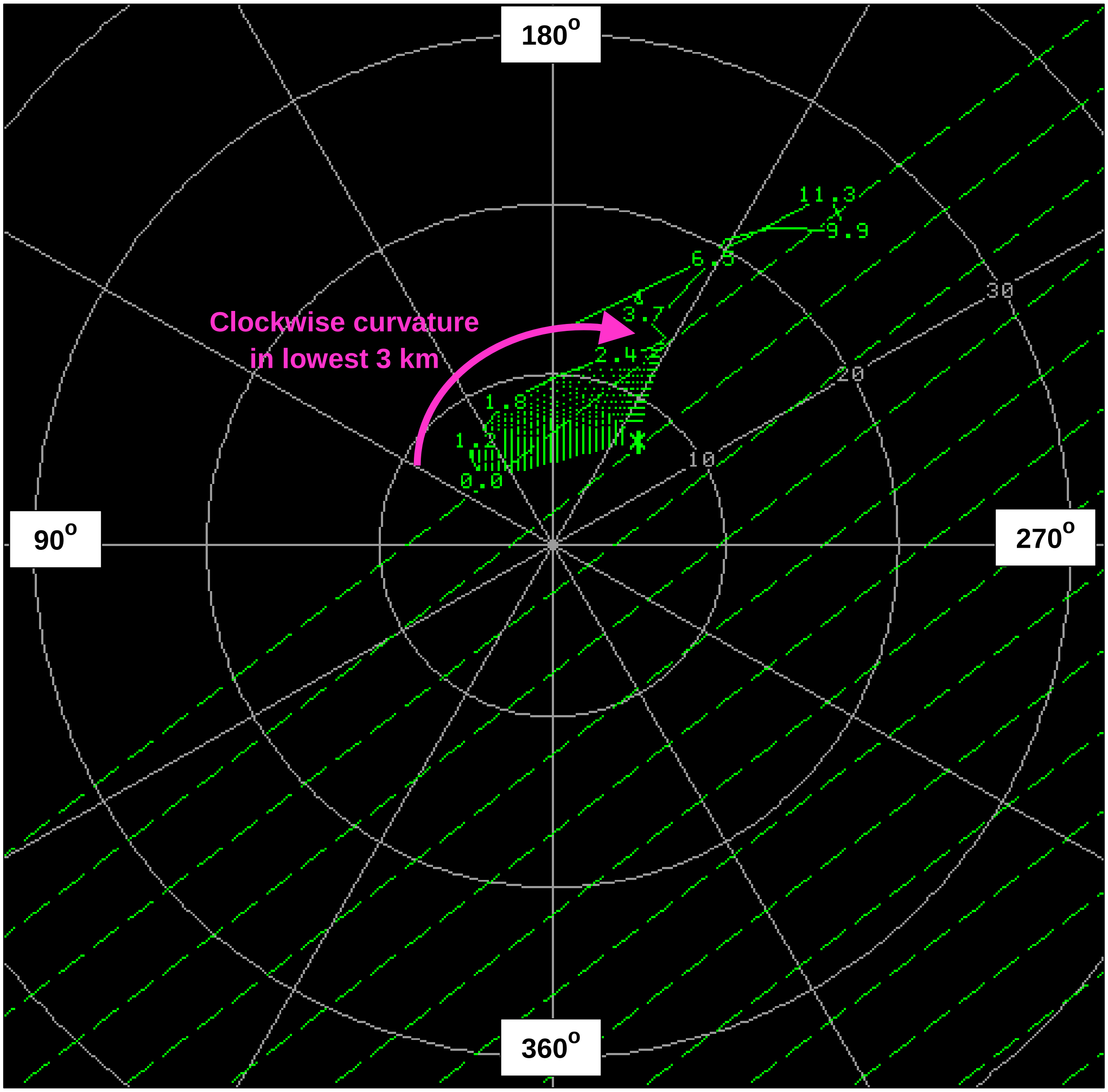

Figure 7 – NAM12 hodograph progged at 18/2100 UTC (KMSO).

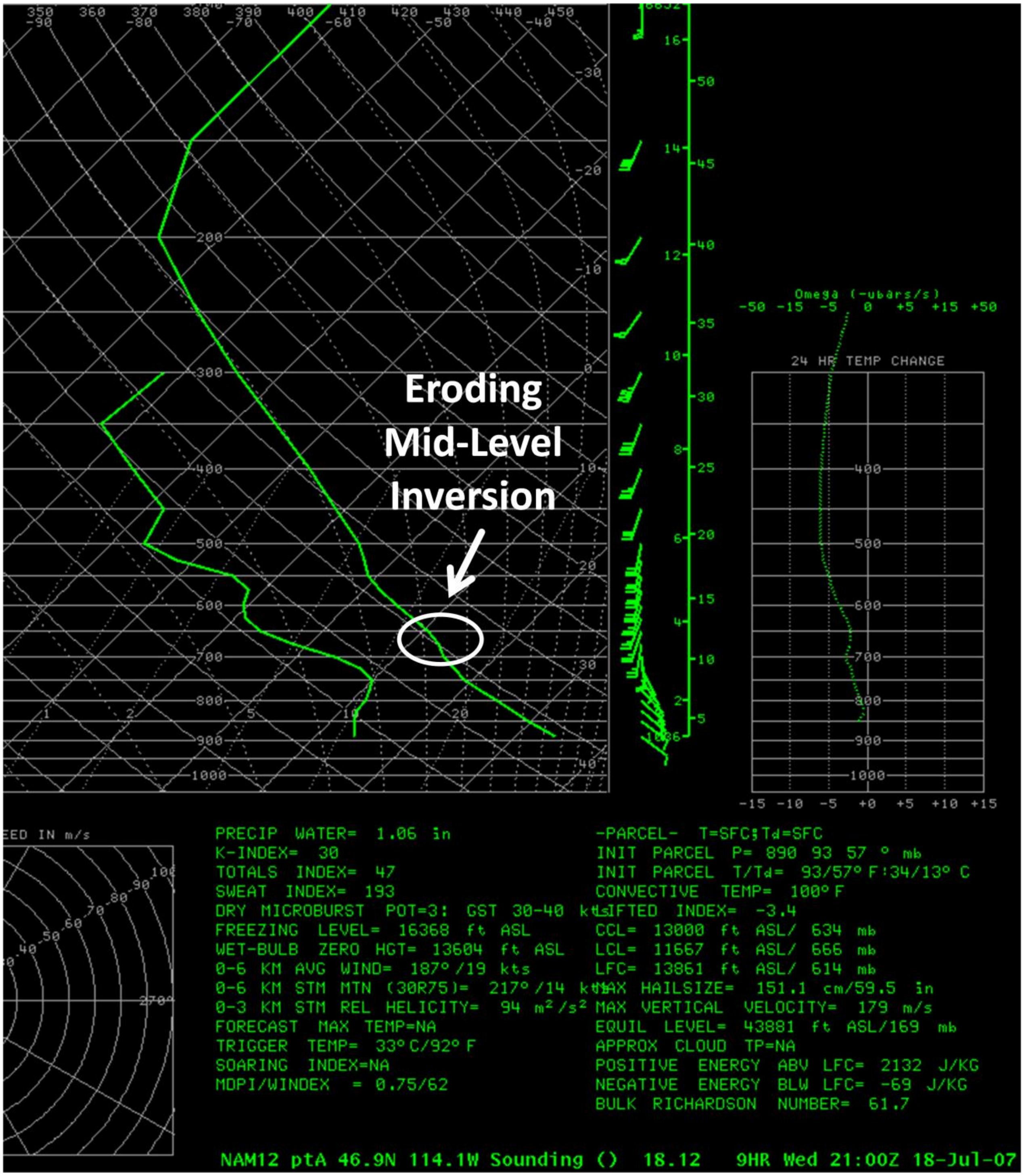

Figure 8 – KMSO NAM12 sounding progged at 18/2100 UTC. Model data suggests that a weak, mid-level inversion would erode during the late afternoon.

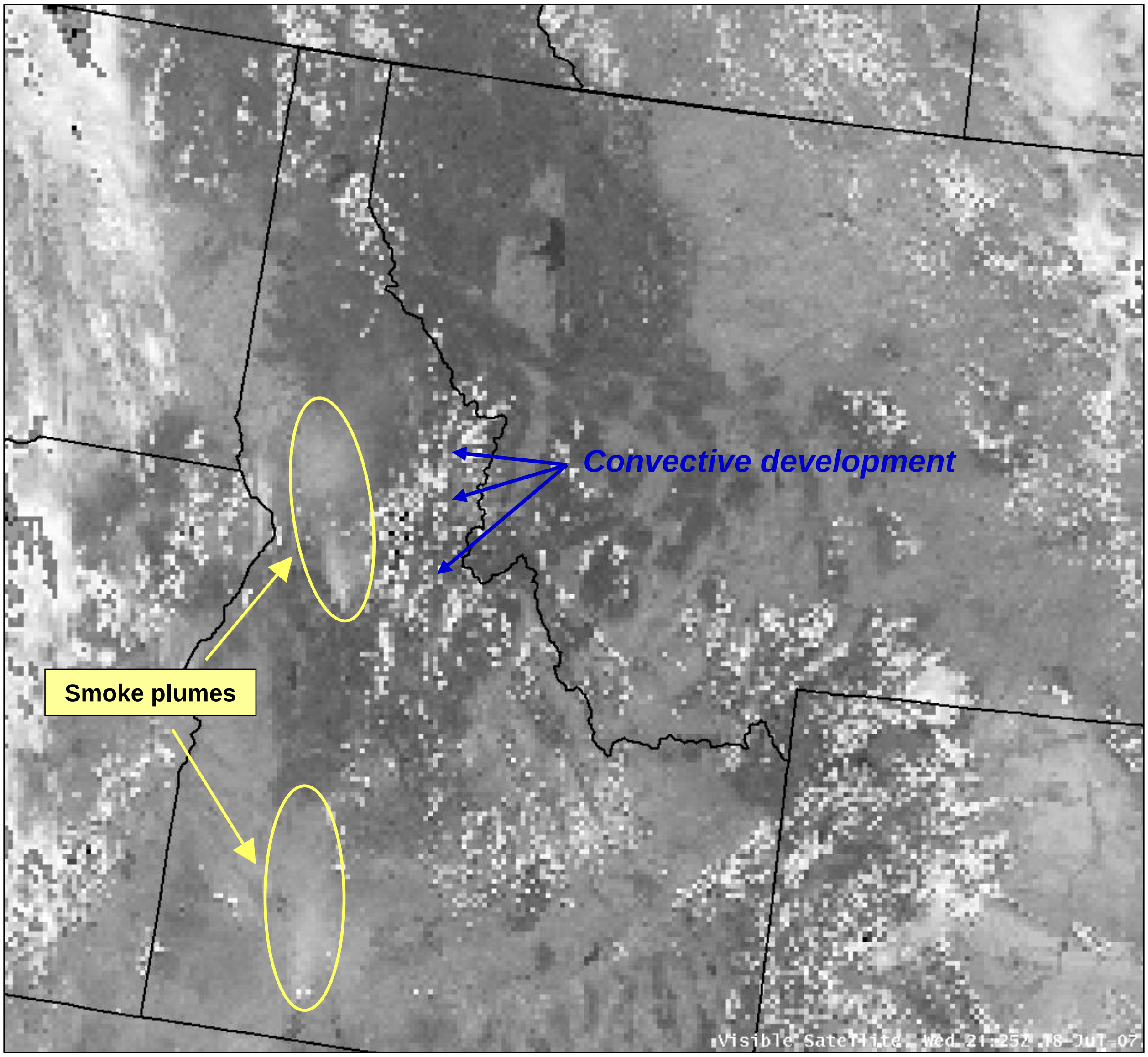

Figure 9 – Visible satellite image showing rapid convective cloud development at 18/2125 UTC over central Idaho. Note the lack of smoke plume activity during the active 2007 Northern Rockies fire season. This would allow for maximum daytime heating to be realized on this day.

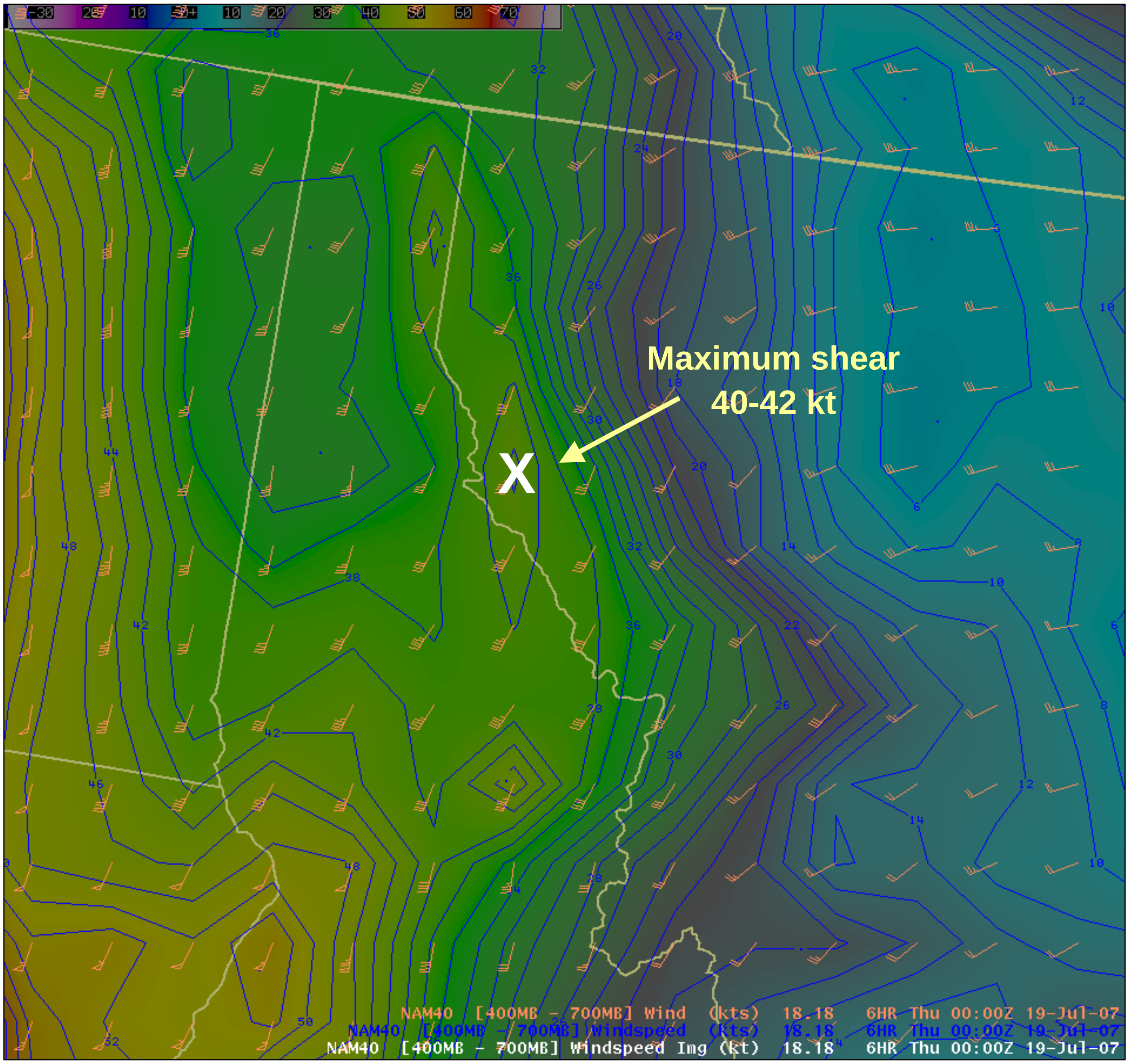

Figure 10 – NAM12 estimated shortwave location (white X) over western Montana as seen on 700-400 mb vertical wind shear progged at 19/0000 UTC.

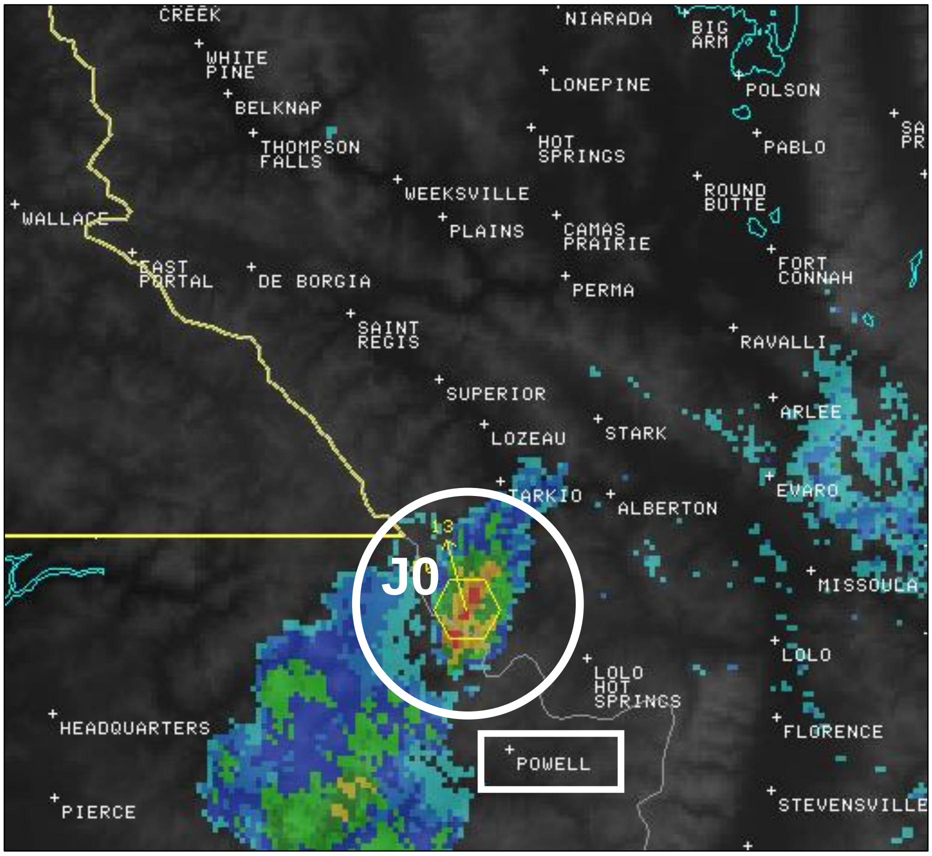

Figure 11 – Initiation of J0 storm cell north of Powell, ID at 18/2322 UTC as seen on this composite reflectivity image with a black and white topographic background. Gray areas represent higher elevations.

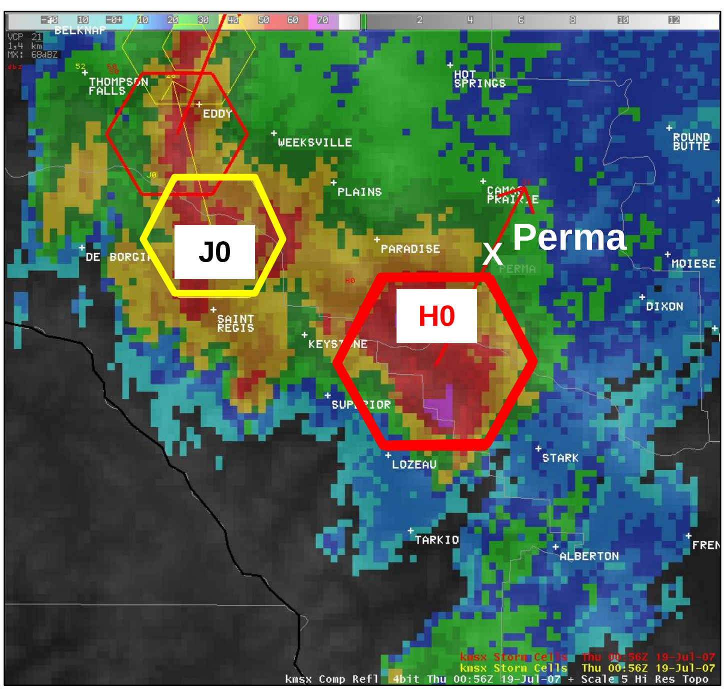

Figure 12 – Merged cell H0 (now the Polson supercell) at 19/0056 UTC southwest of Perma, MT.

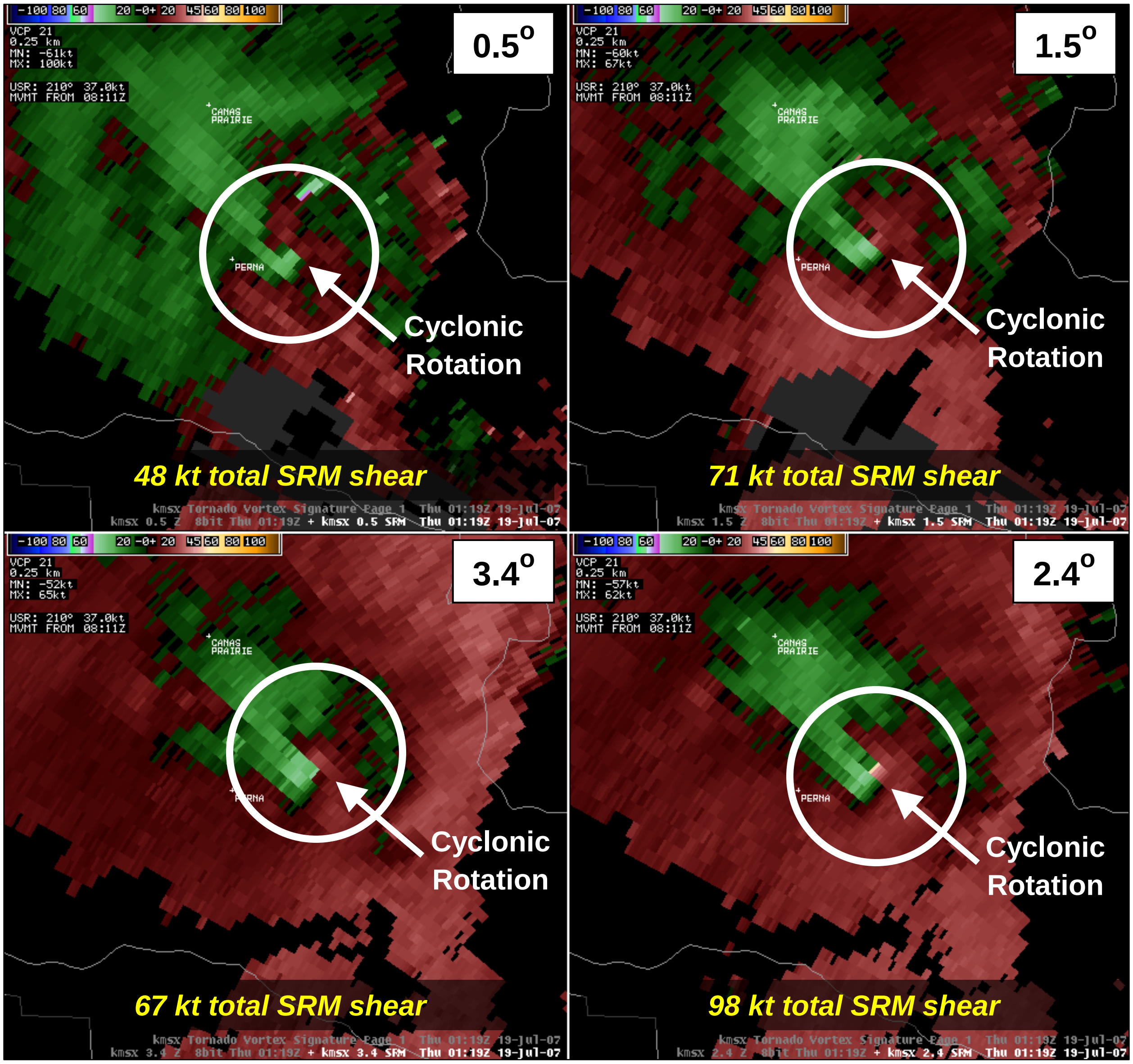

Figure 13 – Low-level 4-panel image of SRM data at 19/0119 UTC. This 4-panel image shows cyclonic rotation and horizontal gate-to-gate total shear values at each radar elevation angle. WSR-88D KMSX is located in the lower right hand corner of each elevation image.

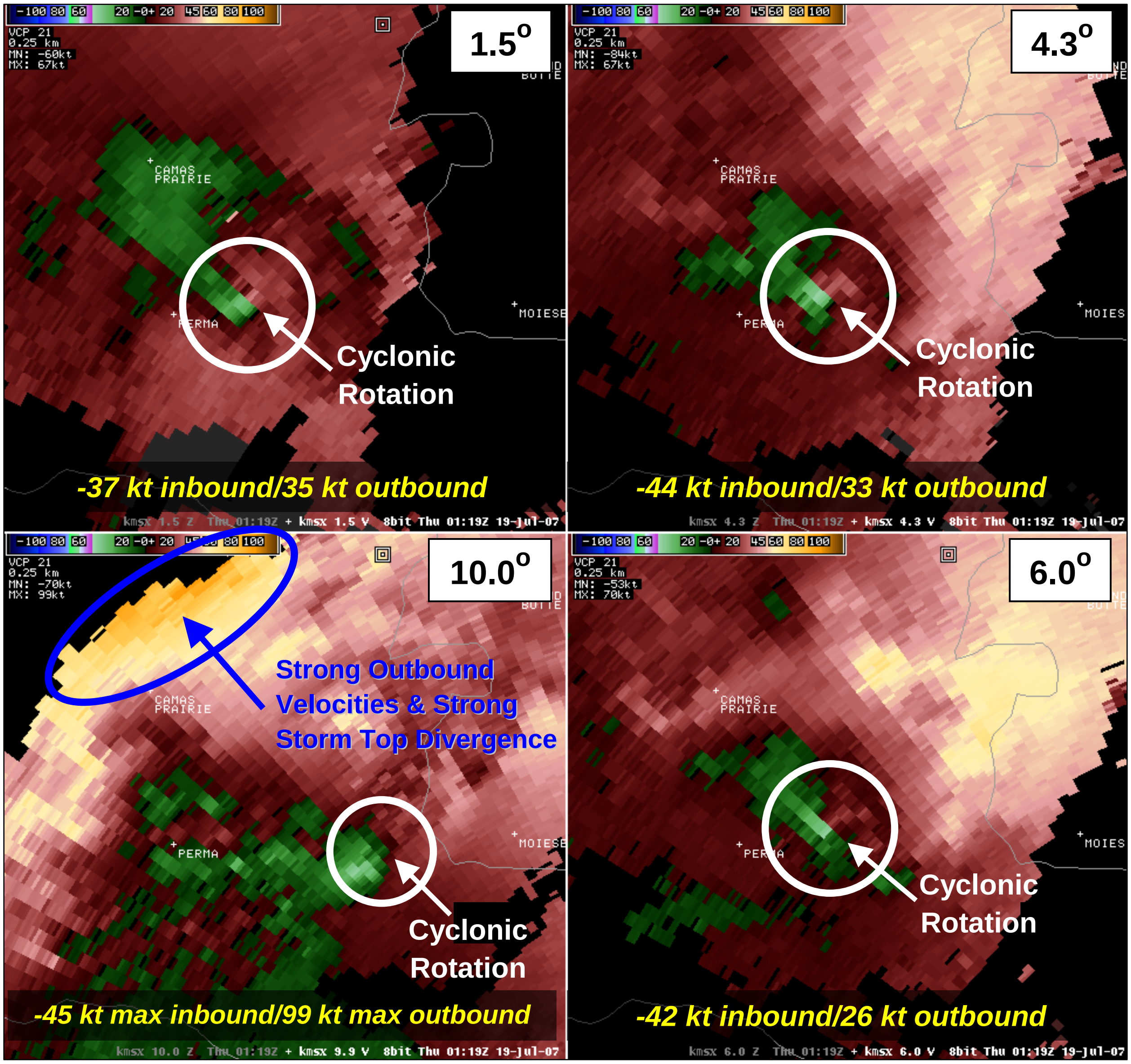

Figure 14 – 4-panel base velocity image at 19/0119 UTC. This image shows cyclonic rotation in the low and mid-levels of the Polson supercell, as well as inbound (-) and outbound (+) velocity values. Cyclonic rotation near the storm's core and strong storm top divergence can be seen on the 10.0^{o} elevation angle (lower left hand corner). WSR-88D KMSX is located in the lower right hand corner of each elevation image.

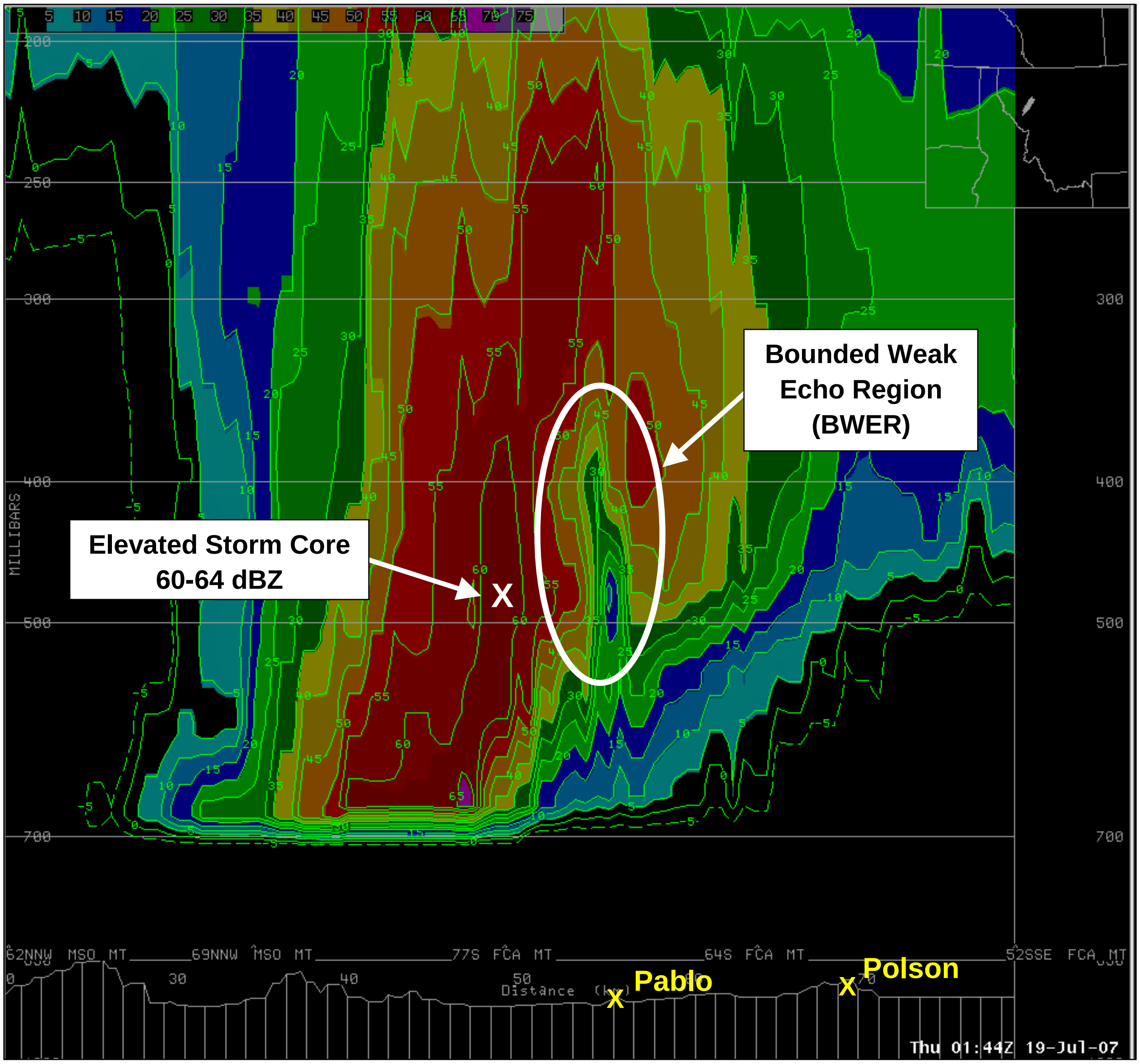

Figure 15a – Reflectivity cross section of the Polson supercell at 19/0144 UTC. A Bounded Weak Echo Region (BWER) is seen just above 400 mb. Note the location and strength of the elevated storm core at this time (white X). A WSR-88D algorithm Tornadic Vortex Signature (TVS) alarm was alerting during this radar volume scan.

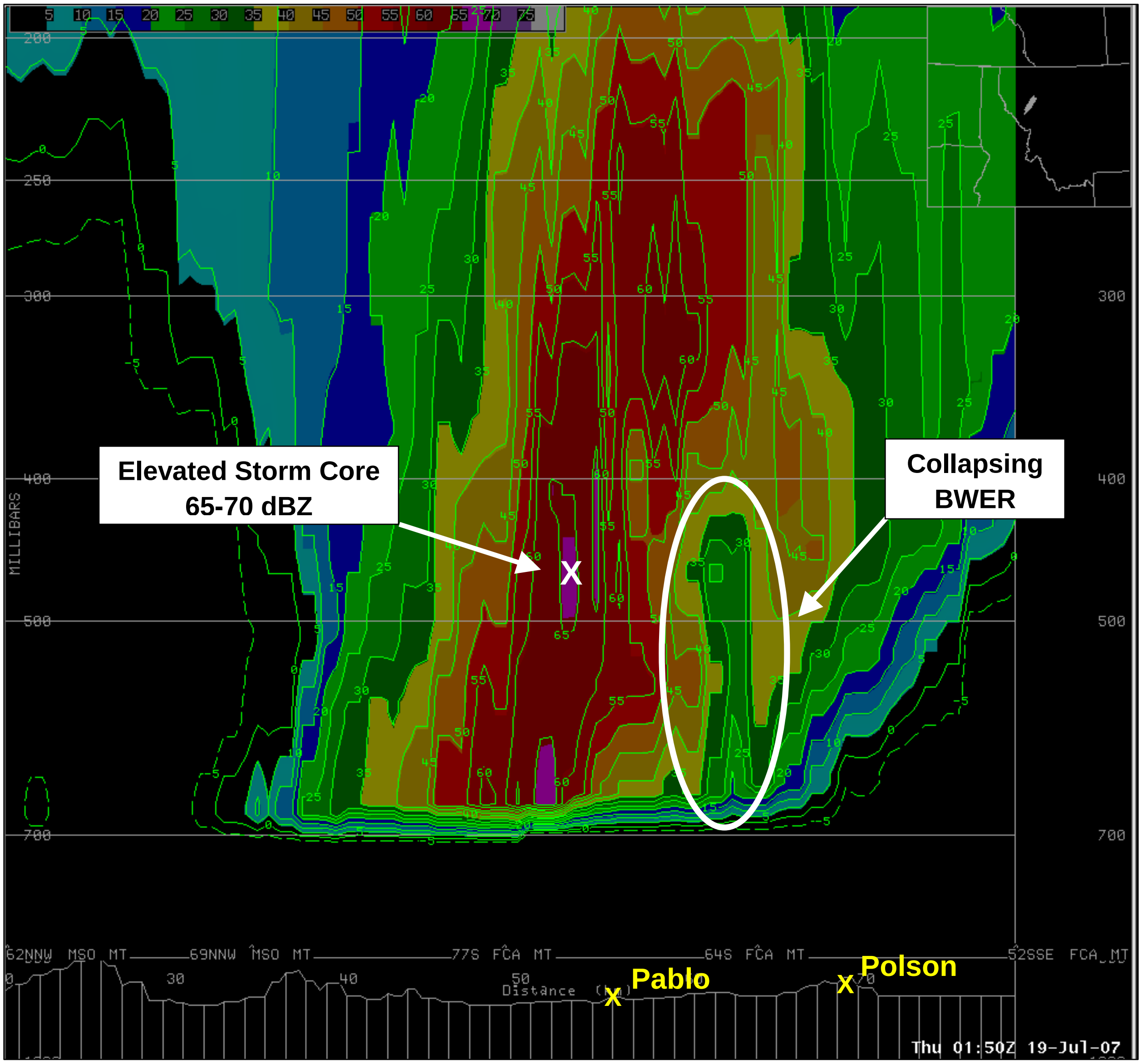

Figure 15b – Reflectivity cross section of the Polson supercell at 19/0150 UTC. The BWER has descended and weakened below 400 mb, while the elevated storm core (white X) is intensifying during this time. A WSR-88D algorithm TVS alarm was alerting during this radar volume scan.

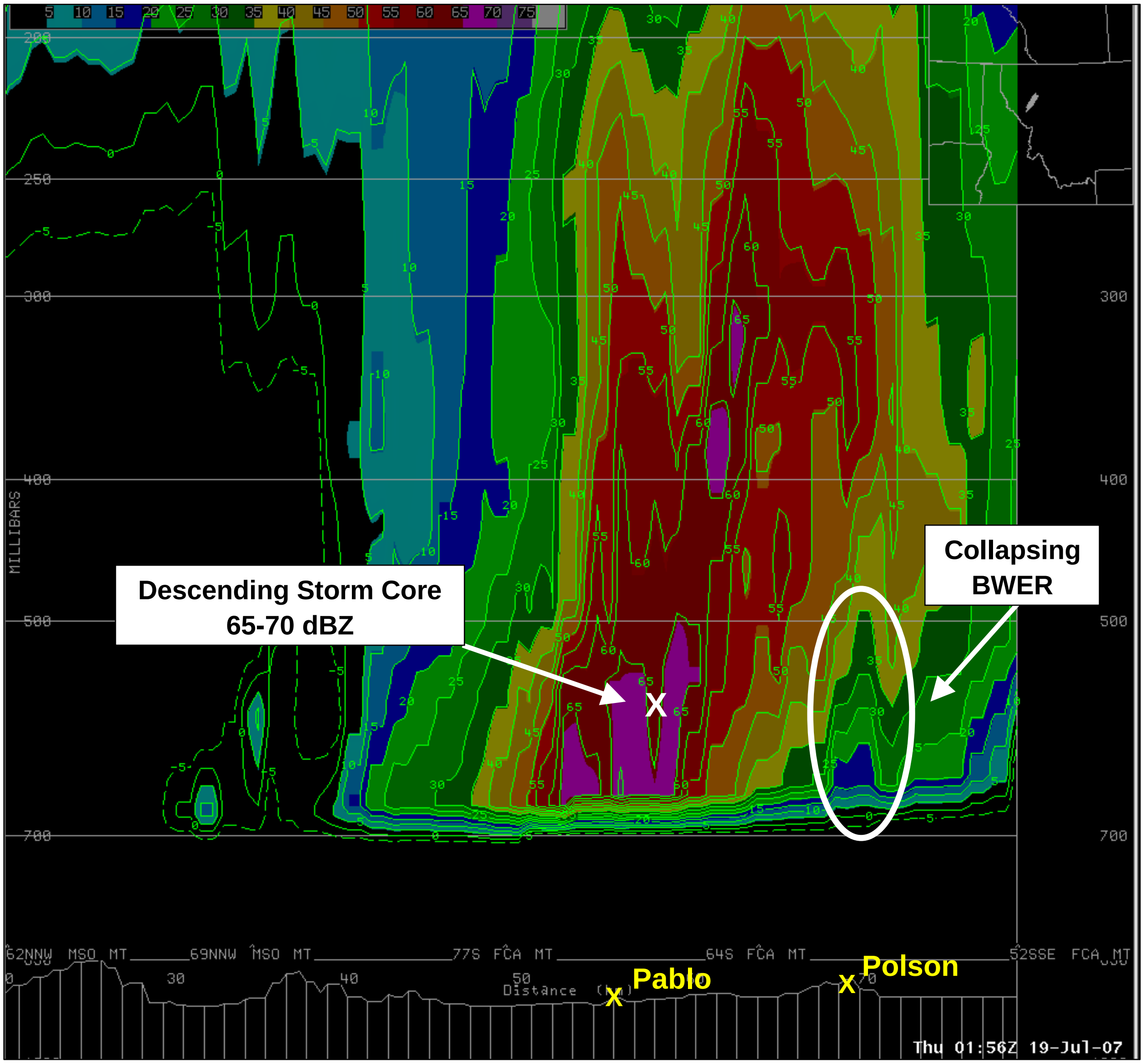

Figure 15c – Reflectivity cross section of the Polson supercell at 19/0156 UTC. The BWER has almost fully collapsed over Polson, MT. Meanwhile, the supercell's storm core (white X) remains intense and continues to descend toward the surface. This is strong evidence of a microburst occurring during this time. Straight-line wind damage was reported in the area west of Pablo.

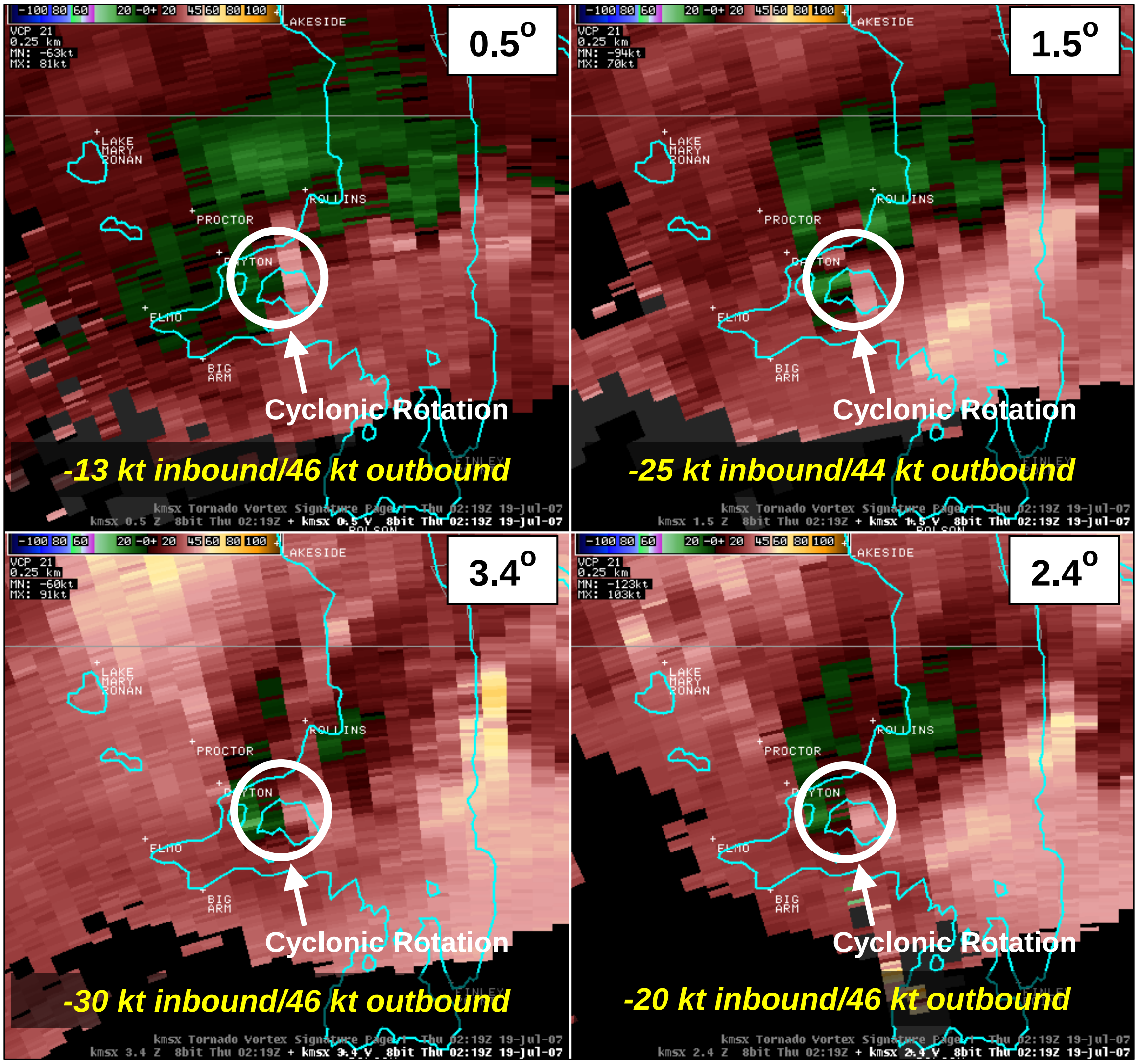

Figure 16 – Low-level 4-panel image of base velocity data at 19/0219 UTC, which shows cyclonic rotation throughout the low and mid-levels of the storm. Inbound (-) and outbound (+) velocities listed in this graphic are not horizontal gate-to-gate shear values; they are maximum inbound and outbound values in the area of strongest cyclonic rotation (white circle). Funnel clouds and a waterspout over Flathead Lake were reported during this time.

Figure 17 – Collapsing downdraft and subsequent microburst near Somers, MT between 19/0230 and 19/0300 UTC as the Polson supercell and mesocyclone rapidly dissipates (photo received from the public).

Figure 18 – Polson supercell storm reports. Color-coded stars indicate type of damage received. Yellow represents hail. Orange represents wind damage. Red represents waterspouts.

Figure 19 – Structural damage to a metal barn structure four miles west of Pablo, MT (photo courtesy of Bryan Henry).

Figure 20 – Sailboat pushed onshore between Elmo, MT and Rollins, MT by straight-line winds associated with the Polson supercell (photo courtesy of Lake County Department of Emergency Services).

Figure 21 – Metal silo knocked over and damaged near Somers, MT (photo courtesy of Bryan Henry).

Figure 22 – Structural damage to a metal barn near Somers, MT (photo courtesy of Bryan Henry).

Figure 23 – A four to five foot diameter cottonwood tree completely uprooted near Somers, MT. As a reference, NWS forecaster Mark Loeffelbein (seen in this photo) is 6 feet 3 inches tall. The residence here was not damaged by the downed tree or other debris (photo courtesy of Bryan Henry).